Astronomy & Astrophysics manuscript no. rvvar_2b
April 25, 2019

Spectroscopic orbits of nearby stars

J. Sperauskas[1], V. Deveikis[1], and A. Tokovinin[2]

[1] Vilnius University Observatory, Saulėtekio al. 3, 10257 Vilnius, Lithuania
e-mail: julius.sperauskas@ff.vu.lt
[2] Cerro Tololo Inter-American Observatory, Casilla 603, La Serena, Chile
e-mail: atokovinin@ctio.noao.edu

Received 2019; accepted

ABSTRACT

Aims. We observed stars with variable radial velocities to determine their spectroscopic orbits.
Methods. Velocities are presented of 132 targets taken over a time span reaching 30 years. These were measured with the correlation radial velocity spectrometers (1917 velocities) and the new VUES echelle spectrograph (627 velocities), with a typical accuracy of 0.5 and 0.2 km s^{-1} , respectively.
Results. We derived spectroscopic orbits of 57 stars (including 53 first-time orbits), mostly nearby dwarfs of spectral types K and M, with some being Hipparcos astrometric binaries. Their periods range from 2.2 days to 14 years. Comments on individual objects are provided. Many stars belong to hierarchical systems containing three or more components, including 20 new hierarchies resulting from this project. The preliminary orbit of the young star HIP 47110B has a large eccentricity $e = 0.47$ despite having a short period of 4.4 d; it could still be circularizing.
Conclusions. Our results enrich the data on nearby stars and contribute to a better definition of the multiplicity statistics.

Key words. Binary stars – Nearby stars

1. Introduction

The solar neighborhood is the best-studied part of the Galaxy. Yet, it is still a site of active research and new discoveries. While the *Gaia* satellite is improving the census of our stellar neighbors, several observational campaigns target nearby stars in search of exo-planets. Studies of specific stellar populations, such as young associations or metal-poor stars, inevitably focus on the nearest objects. Last but not least, the solar neighborhood is the benchmark for stellar multiplicity statistics.

Here we report the results of the large campaign of radial velocity (RV) measurements, which started three decades ago, before the *Hipparcos* mission, targeting mostly nearby low-mass stars. The aims and main results of this campaign are presented by Sperauskas et al. (2016), where the stars with constant RVs are featured. Here we focus on the remaining objects with variable (or supposedly variable) RVs. Our goal is the determination of spectroscopic orbits of these stars.

Radial velocity monitoring over several years is very efficient in discovering spectroscopic binaries (SBs); only a few (e.g., three) RV measurements are needed to detect the RV variability or double lines. However, determination of orbits of these SBs requires substantial follow-up efforts. For example, the Geneva-Copenhagen Survey (GCS, Nordström et al. 2004) discovered hundreds of SBs, but their orbits remain for the most part unknown or unpublished. This leads to uncertainties in the study of stellar multiplicity, namely in the distribution of periods and mass ratios of nearby solar-type stars (Tokovinin 2014).

Nowadays, hundreds of thousands of RV measurements come from *Gaia* (Gaia Collaboration et al. 2018) and ground-based surveys such as APOGEE (e.g., Albareti et al. 2017), RAVE (Steinmetz et al. 2006), or LAMOST (Zhao et al. 2012). However, some SB orbits require either a long time span or a frequent cadence, which are not provided by the automatic surveys. So far, only *Gaia* offers the full-sky coverage, but it has not yet provided individual RV measurements suitable for orbit calculation. Moreover, treatment of double-lined systems and complex cases such as triples by the *Gaia* pipeline may be problematic. Our results are therefore unlikely to become obsolete in the near term.

The results of our observations are useful in many ways. They provide previously unknown periods and mass ratios of low-mass binaries in the solar neighborhood that serve to improve the multiplicity statistics. The recent discovery of the strong dependence of the close-binary fraction on metallicity (Moe et al. 2018) puts such efforts in a new context. Several binaries detected by *Hipparcos* accelerations have their spectroscopic orbits determined here. Similarly, this dataset will help in the interpretation of astrometric accelerations measured by *Gaia*, as our time coverage is much longer than the duration of this mission. Finally, some objects in our sample present special interest for various reasons, making the knowledge of their orbits essential.

The objects of this study are presented in Sect. 2. Section 3 covers the instruments and methods used to derive the orbits. Our results, namely the orbits and comments on individual objects, are given in Sect. 4. Finally, our conclusions are presented in Sect. 5.

2. The observed sample

The core of the observing program is the survey of K- and M-type dwarfs featured in the McCormic catalog (see a review in Upgren & Weis 1989) and in the catalog of nearby stars (Gliese & Jahreiß 1991). Stars with constant RVs presented by Sper-

Article published by EDP Sciences, to be cited as https://doi.org/10.1051/0004-6361/201935346

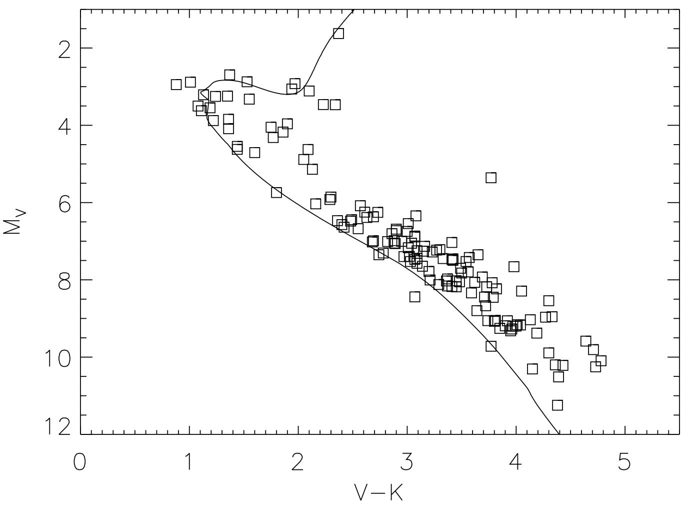

Fig. 1. Color-magnitude diagram of stars from Table 1. The line is a 4 Gyr isochrone for solar metallicity from Bressan et al. (2012). The discrepant point is caused by the erroneous parallax of BD−08 2689.

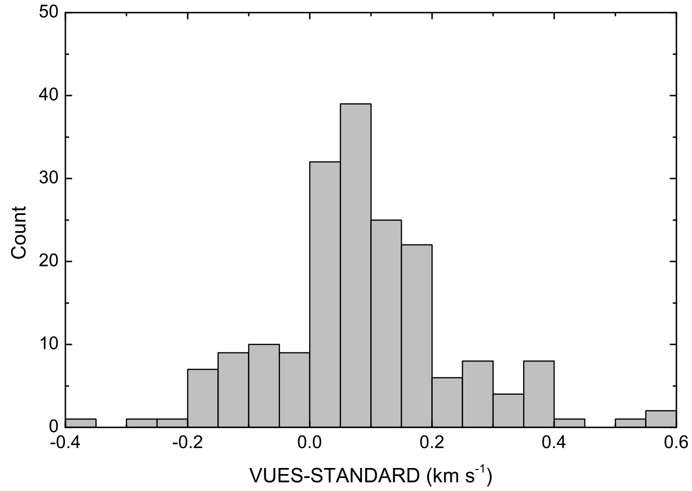

Fig. 2. Radial velocities of IAU RV standard stars measures by VUES. The histogram of the RV difference is plotted.

auskas et al. (2016) were used to study the local kinematics. Objects with variable RVs studied here were monitored more extensively for orbit determination. The spectroscopic survey of nearby K dwarfs by Halbwachs et al. (2003, 2018) pursued similar goals, and six of their objects are common to our sample. In addition to the nearby dwarfs, we monitored several other objects with variable RVs and present their orbits here. In particular, our program was augmented by the *Hipparcos* stars with astrometric accelerations (Makarov & Kaplan 2005) with the aim being to establish their periods.

Table 1 contains the object list and the synopsis of our results. Its first column gives common identifiers (HIP numbers are preferred, with HD or BD as the second choice), and the following two columns give the equatorial coordinates for J2000. Then follow the visual magnitude V, parallax ϖ, and spectral type. These data were recovered from Simbad. Almost all parallaxes come from the *Gaia* DR2 (Gaia Collaboration et al. 2018). The remaining columns of Table 1 summarize our results. The variability is coded as C – constant, V – variable, s2 – double-lined, S1, S2, or S3 – single- , double-, and triple-lined binaries with orbits determined here. Then follow the number of RV measurements N, their time span ΔT, and the weighted mean velocity $\langle RV \rangle$. For binaries with orbits, $\langle RV \rangle$ is the center-of-mass velocity. The last two columns contain the statistics explained below.

To give an idea of the stars studied here, we place them on the color-magnitude diagram in Fig. 1. Most stars are low-mass dwarfs, although hotter F-type stars and giants are also present in our sample. We reiterate that at the start of our program, the trigonometric parallaxes were not available, and some stars classified spectroscopically as dwarfs turned out to be giants. The median parallax is 25 mas, meaning that half of the objects are located within 40 pc of the Sun. The closest, HIP 29295, has a distance of only 5.7 pc. On the other hand, 16 objects (mostly giants) have parallaxes less than 5 mas.

3. Observations and data processing

3.1. Instruments

The first RV measurements reported here date back to February 1988. They were made using the correlation radial-velocity meter (RVM) installed at the 1 m Lithuanian telescope at Mt. Maidanak, in Uzbekistan (see e.g., Tokovinin 1992). Like the CORAVEL instrument (Baranne et al. 1979), it scans the echelle spectrum over the physical mask with slits corresponding to individual spectral lines, accumulates the transmitted flux as a function of the relative shift, and determines the RV by approximating the cross-correlation curve with one or several Gaussian curves.

Starting from 1998, a similar CORAVEL-type instrument constructed at the Vilnius observatory became operational. It worked mostly at the 1.65 m telescope of the Moletai observatory, although several trips to other telescopes were made. The instrument and observing runs are further described by Sperauskas et al. (2016). This latter publication also gives a thorough analysis of the RV zero points and accuracy by comparing results to several lists of RV standards. In the following, we refer to both instruments as CORAVELs, without making distinction between them.

In 2015, the CORAVEL in Moletai was replaced by the modern fiber-fed echelle spectrometer VUES (Jurgenson et al. 2016). It covers the spectral range from 400 to 880 nm with a resolution from 30000 to 60000. In this program we used the lowest resolution of 30,000. The first RV measurement with VUES reported here was made on November 26, 2015 (JD 2457352). The spectrum recorded by the CCD detector is extracted and calibrated in the standard way. The RV is determined by numerical cross-correlation of this spectrum with a binary mask, emulating the CORAVEL method in software. Compared to CORAVEL, the RVs delivered by VUES are more accurate; their rms residuals from the orbits are typically from 0.2 to 0.3 km s^{-1} . The RV zero point is controlled by observations of the IAU RV standards (Fig. 2). The systematic RV offset of VUES is less than 0.1 km s^{-1} .

3.2. Detection of variable RVs

For each star, the mean radial velocity $\langle RV \rangle$ was computed with weights inversely proportional to the squares of the measurement errors. The errors of the CORAVEL RVs σ_i were used as listed, while the errors of the RVs measured by VUES were augmented by adding quadratically 0.2 km s^{-1} because the internal errors determined by the dip fitting do not account for other error sources such as wavelength calibration and instrument stability.

Table 2. Radial velocities (fragment)

Name	JD +2400000	RV (km s^{-1})	σ (km s^{-1})	Inst.	a/b
HIP 96	55470.486	−11.70	0.60	C	
HIP 96	55485.410	−11.60	0.50	C	
HIP 3428	58387.512	−1.09	0.42	V	a
HIP 3428	58387.512	−14.29	0.53	V	b

The weighted rms deviation from the mean, σ_V, is computed as

$$\sigma_v = \sum_{i=1}^{N} (RV_i - \langle RV \rangle)^2 \sigma_i^{-2} \ / \ \Sigma_{i=1}^{N} \sigma_i^{-2}. \quad (1)$$

The first term of this equation, divided by the number of measurements $N-1$, gives the normalized $\chi^2/(N-1)$ statistic, which has a mathematical expectation of one for a constant RV and realistic errors σ_i. The statistics σ_V and $\chi^2/(N-1)$ are given in the last two columns of Table 1, except for the stars with computed orbits. The large values $\chi^2/(N-1) > 100$ are replaced by 99. For multi-lined systems, the statistics are computed for the primary component.

3.3. Orbit calculation

Spectroscopic orbits were determined with the help of the IDL code `orbit.pro`.[1] Individual RVs are weighted in proportion to σ_i^{-2}. However, the errors are artificially increased when RVs are deduced from partially blended dips and in other instances where the residuals strongly exceed the errors. In a few cases where the spectroscopic pair is also resolved, we fitted combined spectro-visual orbits using the same code. The errors of RVs and positional measurements are balanced in the sense that the normalized statistic χ^2/N for each type of data should be close to one. Finally, orbits of triple systems were fitted using an extension of this code called `orbit3.pro` and described by Tokovinin & Latham (2017); this is also available online.

4. Results

4.1. Individual RVs

Table 2, published in full at the CDS, lists individual RV measurements, a total of 1917 velocities obtained with CORAVEL, and 627 velocities measured with VUES. Its first column is the object name (same as in the object list). Then follow the Julian date, RV, its internal error, and the instrument code (V for VUES and C for CORAVEL). For double-lined binaries, the last column distinguishes the primary and secondary components by the letters a and b, respectively.

4.2. Spectroscopic orbits

The orbital elements and their errors are listed in Table 3 in standard notation. For circular orbits, we fixed the eccentricity e and the argument of periastron ω. The second-to-last column gives the weighted rms residuals for the primary component or for both components of double-lined (SB2) binaries. The spectroscopic masses $M_{1,2} \sin^3 i$, that is, the minimum masses, are provided for SB2s in the last column. For the single-lined pairs (SB1s), this column contains the minimum secondary mass estimated from the orbit after adopting a reasonable guess for the primary mass.

The RV curves of spectroscopic binaries are given in Figs. 3–5. In each panel, the horizontal axis is the orbital phase from 0 to 1.5 (the first half-period is repeated), the vertical axis is the RV in km s^{-1} . The RV curves of the primary and secondary components are plotted in full and dashed lines, respectively, while the squares and triangles denote the measurements. In some plots, crosses denote RVs with reduced weights.

4.3. Comments on the individual objects

This section provides notes on individual stars and stellar systems from our list. Hierarchical systems with three or more components are also featured in the Multiple-Star Catalog (MSC, Tokovinin 2018). Several objects with subsystems discovered here are added to the MSC. Data on visual components are taken from the Washington Double Star catalog (WDS, Mason et al. 2001) and from the MSC.[2] Unknown periods of visual binaries are estimated crudely from projected separations assuming that they equal the semimajor axis. Similary, the semimajor axes of spectroscopic binaries are estimated from their periods, using known distance and a guess of the masses of the components. Information on astrometric accelerations detected by the *Hipparcos* mission comes from the paper by Makarov & Kaplan (2005).

HIP 96 (BD+13 5195, M0.5V, 43 pc). This visual triple system consists of the 11″ pair A,B and the 0.″2 subsystem Aa,Ab with $P \sim 25$ yr. All components are M-type dwarfs. We find that the RVs of both A and B are slowly variable. This is expected for A, which is a close pair; the component B may also host a low-mass companion.

HIP 374 (HD 225220), a K0 giant, is the main component A of the hierarchical system located at a distance of 200 pc. The outer pair A,D has a 95.″3 separation; A,B is a visual binary with $P = 545$ yr. The main sequence star D (TYC 2267-1300-1, probably of F9V spectral type) is found here to be an SB1 with $P = 68$ d. This is therefore a quadruple system of 2+2 hierarchy. The star C = HIP 375, listed in the WDS, is optical, as evidenced by its proper motion (PM), different parallax, and the RV measured here.

HIP 1412 (K7V, 32 pc) has a large RV variation, but no orbit can be derived yet from our six RVs.

HIP 3428 (BD+23 97, K7, 45 pc) is a double-lined twin binary with $P = 97$ d and the mass ratio $q = 0.96$. Interestingly, it has an astrometric acceleration, and therefore is likely a triple system. However, residuals to the spectroscopic orbit do not show any slow trends.

HIP 5110 (HD 6440, 27 pc) is a 6.″1 physical binary STF 87 with an estimated period of ∼2 kyr. We discover RV variability of the component B, of K8V spectral type. Considering also the 2.5 km s^{-1} RV difference between A and B, presumably caused by the orbital motion of Ba,Bb, we believe that this is a triple system.

HD 8691 (G0, 50 pc) is a high-PM star and an SB1 with $P = 581$ d, with a low-mass secondary.

HIP 9867 (GJ 84.2, M0V, 19 pc) is a high-PM star and a double-lined pair with $P = 897$ d and unequal correlation dips. The WDS lists three visual companions, all optical. Eclipses are reported by Malkov et al. (2006).

[1] The code can be downloaded from `http://www.ctio.noao.edu/~atokovin/orbit/`

[2] See the latest version at http://www.ctio.noao.edu/˜atokovin/stars.

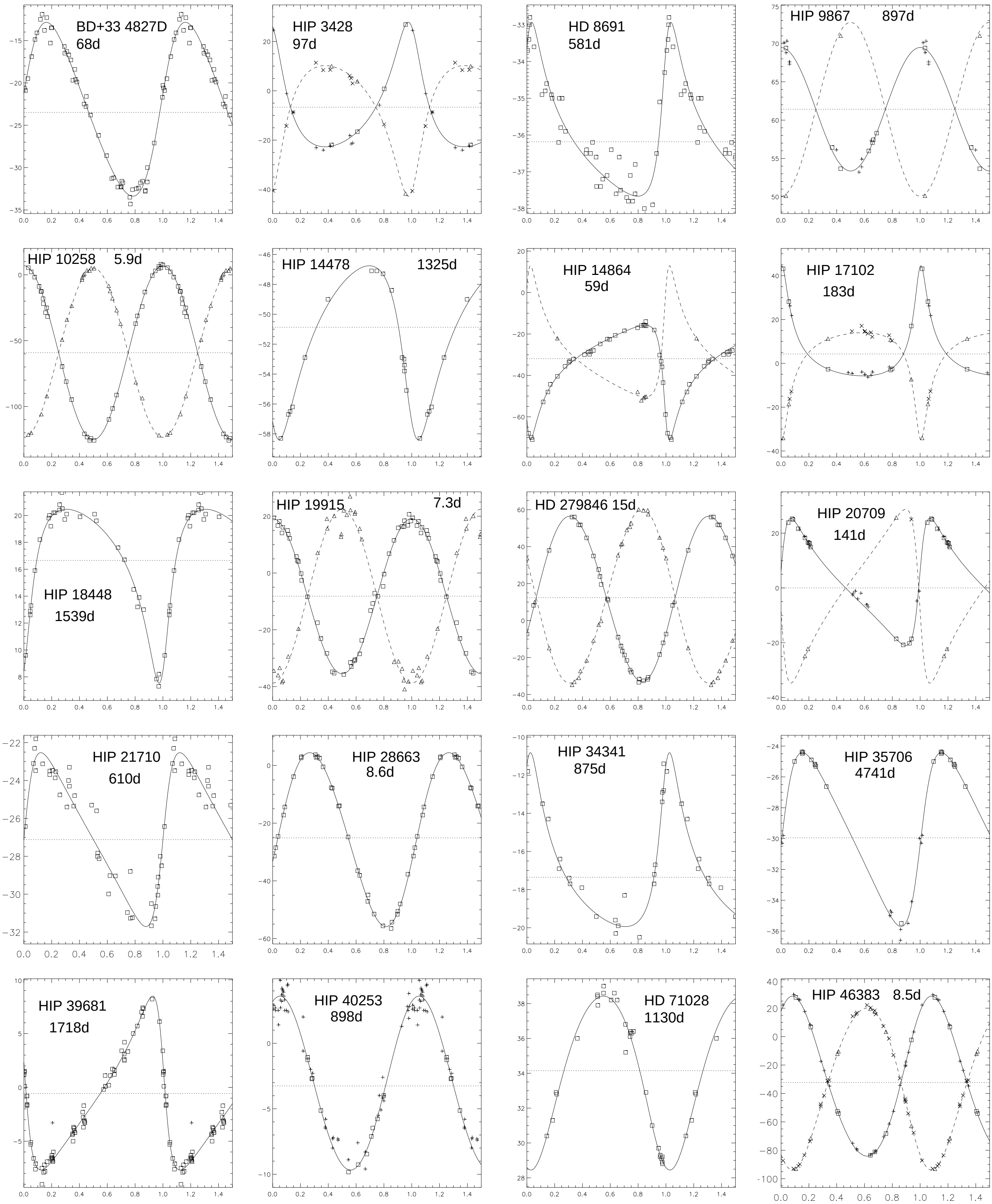

Fig. 3. RV curves. Object names and approximate periods are indicated. In each plot, the horizontal axis is the orbital phase, the vertical axis is the RV in km s^{-1} . The RV curves of the primary and secondary components are plotted in full and dashed lines, respectively, while the squares and triangles denote the measurements. In some plots, crosses denote RVs with reduced weights.

HIP 10258 (BD+03 301, K5, 47 pc) is a chromospherically active double-lined binary with P = 5.9 d and a mass ratio q = 0.93. Its visual companion at 25″(SKF 1518) shares common parallax, PM, and RV.

BD+49 646 (unknown spectral type, 53 pc) has double correlation dips, but we have not derived its orbit from the eight spectra. It is an X-ray source.

HIP 11437 (AG Tri, K7V, 41 pc) is a young chromospherically active star in the β Pictoris moving group (Messina et al. 2017); it has been extensively covered in the literature. We found a constant RV of 6.0 km s^{-1} (see also Sperauskas et al. 2016), in agreement with other published studies. The visual companion at 22″ is physical.

HIP 12787 (MCC 401, M0Ve, 49 pc) is a triple system with the outer 21″physical binary A,C. Its primary component is an astrometric binary, resolved directly in 2015.9 at 0.″25 by Janson et al. (2017); its estimated period is ∼40 yr. The spectrum is double-lined, suggesting existence of a close subsystem, but no orbit is derived. The components A and C are located above the main sequence and belong to the β Pictoris moving group according to Janson et al. The component B at 25″ listed in the WDS is optical.

HIP 13398 (G 36-38, M2V, 23 pc) is a high-PM star, likely with a variable RV.

HIP 13460 (BD+60 585, K3V, 39 pc) is a triple system discussed in the following section.

HIP 14478 (V568 Per, K6, 27 pc) is a triple system. The outer 2.″9 pair A 1572 has an estimated period of ∼600 yr. Its primary component is a single-lined binary with P = 1325 days. The semimajor axis of the inner subsystem is 87 mas and it is detectable astrometrically from the PM difference between *Gaia* and *Hipparcos*.

HIP 14669 (MCC 99, M2V, 17 pc) is a *Hipparcos* visual binary with known orbit, P = 28.3 yr. We see an RV trend by 6 km s^{-1} over 7 years, presumably caused by this orbit.

HIP 14864 (BD+60 637, M0Ve, 25 pc) is a triple system consisting of the 0.″6 binary discovered by *Hipparcos* (period ∼40 yr) and the double-lined subsystem Aa,Ab with P = 59.5 d and q = 0.88, discovered here.

BD+03 480 (V1221 Tau, G0, 83 pc) is a young visual triple system, where the inner 0.″9 binary A 2417BC has been known for a long time (since 1912), while another companion D at 2.″2 was discovered a century later, in 2012, and has not yet been confirmed as physical (it is not found in *Gaia* DR2). Our 11 observations over 13 years show a constant RV of 12.66 km s^{-1} . However, *Gaia* DR2 gives an RV of 18.05 km s^{-1} with an error of 7.26 km s^{-1} , suggesting variability.

HIP 17102 (HD 278874, 39 pc) is a flaring K2V dwarf in a triple system. The outer pair ES 327 has a 15.″5 separation and a long ∼10 kyr period. The secondary star B is located above the main sequence. The main component A is a double-lined binary with P = 183 d and q = 0.96 (the components Aa and Ab are interchanged in our orbit). The inner semimajor axis is 18 mas, so the subsystem Aa,Ab can be resolved. lines were noted by Montes et al. (2018).

GJ 3248 is an M1V dwarf at 16 pc. We suspect that its RV is variable.

HIP 18448 (K0, 149 pc) is a triple system composed of the outer 25″pair LDS 1583 and the inner subsystem Aa,Ab revealed by astrometric acceleration. Here we derive its accurate spectroscopic orbit with P = 4.2 yr. The primary star is a subgiant located above the main sequence, while the component B is below; Chanamé & Ramirez (2012) consider B to be a white dwarf.

HIP 19140 (BD−15 728, K5V, 40 pc) certainly has a variable RV, as well as astrometric acceleration.

HIP 19915 (HD 26872, F8, 166 pc) is a triple system composed of the tight 32-mas interferometric pair YSC 128 with an estimated period of ∼6 yr (no orbit is known yet) and the double-lined subsystem with P = 7.3 days. The inner orbit is seen at large inclination, as evidenced by the small spectroscopic masses $M \sin^3 i$. We could not detect variations of the systemic velocity that might be caused by the visual binary.

HD 279846 (K2, 82 pc) is just a double-lined binary with P = 15.5 days and an accurately determined orbit; q = 0.95.

HIP 20709 (HD 27961, F5, 132 pc) is an interesting hierarchical system where both the outer 82-yr visual orbit and the inner 141-day double-lined orbit, determined here, are known. The spectrum is triple-lined. We fit both orbits simultaneously, accounting for the slow RV drift caused by the visual pair HU 609. The inclination of the spectroscopic pair derived from comparison between the spectroscopic mass $M \sin^3 i$ and the mass estimated from absolute magnitude, is 60°or 120°, while the outer inclination is 122°. The two orbits could therefore be coplanar. The inner semimajor axis is 5 mas, and therefore the system can be resolved with long-baseline interferometers like the CHARA array to measure the relative inclination. The rms scatter of RVs of the visual secondary component, B, is large: 2.3 km s^{-1} . A possible orbit of Ba,Bb with a 1600 d period and an amplitude of 2.3 km s^{-1} can be fitted, reducing the weighted rms to 0.6 km s^{-1} . This tentative orbit is not given here. The minimum mass of the hypothetical component Bb is 0.15 $\mathcal{M}_\odot$.

HIP 21710 (HD 286955, K2, 27 pc) is a nearby three-tier quadruple system. The outer 34″pair A,B (GIC 51) has an estimated period of 23 kyr, the intermediate visual binary Aa,Ab resolved by *Hipparcos* has an orbit with P = 204 yr, and the inner spectroscopic binary has a period of 610 days announced by Halbwachs et al. (2003) and eventually published by Halbwachs et al. (2018). We determined the spectroscopic orbit from our own observations, but publish here more accurate elements derived from the combined data.

HIP 21845 (HD 29696, F8, 115 pc) might have a slow RV variation, although comparison between *Gaia* and *Hipparcos* does not reveal any astrometric acceleration. The visual companion at 29″ listed in the WDS is physical, according to its *Gaia* parallax and the RV of 11.4 km s^{-1} (the first discordant measure of this pair given in the WDS is misleading).

HIP 23550 (HD 32387, G8V, 73 pc) shows an RV trend over 9 years, indicative of a long period; it is an acceleration binary. The RV variability with an rms of 1.8 km s^{-1} was also detected by Niedever et al. (2002).

HIP 24488 (HD 33798, V390 Aur) is a visual binary with a period of 513 yr according to its current (still uncertain) orbit. The *Gaia* parallax of 2.14 mas is erroneous, so the *Hipparcos* parallax of 8.73 mas is adopted, in better agreement with the dynamical parallax from the orbit, 6.0 mas. Fekel & Marschall (1991) studied this lithium-rich, chromospherically active G5III giant and concluded that it is not a spectroscopic binary; they quote an RV of 22.5 ± 0.2 km s^{-1} . We noted doubling of some correlation dips that could be caused by the fast rotation, $V \sin i$ = 29 km s^{-1} . The RVs derived from double dips are ignored here, and the RV is likely constant.

GJ 220 is a nearby M2V dwarf (parallax 51.5±4.6 mas) with a variable RV. We derived a tentative orbit with P = 700d and K_1 = 2 km s^{-1} from the 13 measured RVs. More observations are needed however to constrain our orbit before it can be published. Meanwhile, an orbit with P = 721.4 d was published by Baroch et al. (2018). The pair may have been resolved by *Gaia* because DR2 does not provide its parallax.

HIP 28663 (HD 41028, F4IV, 103 pc) is a single-lined binary with a well-determined orbit of P = 8.55 d and the minimum secondary mass of 0.35 $\mathcal{M}_{\odot}$.

HIP 29295 (HD 42581, GJ 229) is a flaring M1V dwarf located at a distance of 5.8 pc. Its RV is constant over the 15.8 years spanned by our observations. There is extensive literature coverage of the search for exo-planets with precise RVs and photometry and the distant brown dwarf companion GJ 229B detected by imaging.

HIP 29316 (BD+10 1032) is an M3V nearby (11 pc) close visual binary KAM 1 with an estimated period of ∼20 yr. *Gaia* DR2 does not provide astrometry for this resolved source. The RV is variable, possibly because of the visual orbit. The WDS companion C at 13″ is optical.

HIP 30269 (HD 44517, F5V, 311 pc) has a large-amplitude RV variation discovered by Nordström et al. (2004), but a yet unknown orbit.

HIP 33560 (HD 51849, K4V, 22.5pc) is a visual triple system composed of the 50″outer pair AB,C and the 0″.6 inner pair A,B discovered by *Hipparcos* with an estimated period of ∼50 yr but a yet unknown orbit. We suspect RV variability that might be caused by motion in the visual pair. The RV trend is also detected by Halbwachs et al. (2018). The star is featured in Sperauskas et al. (2016).

HIP 34341 (BD+03 1552, K5V, 26 pc) is a single-lined binary with P = 875 d, as well as an astrometric binary.

HIP 35706 (BD+68 474, K5V, 42 pc) has a long period of 13 years, fully covered by our RV data. The minimum mass of the secondary is rather large, 0.5 $\mathcal{M}_{\odot}$, and its lines are likely blended with those of the primary, reducing the RV amplitude. It is also an astrometric binary.

HIP 36758 (BD+39 1967, F8, 168 pc) might have a variable RV, although our 11 measurements are not conclusive.

HIP 38195 (HD 63207, G 111-38, G5, 111 pc) is a three-tier visual quadruple system with separations of 109″, 2″.2, and 0″.084. It is metal-poor. One of our ten RVs deviates from the rest, suggesting variability. However, Latham et al. (2002) found a constant RV of 71.61 km s^{-1}, so the existence of a spectroscopic subsystems is unlikely. The inner pair has an estimated period of ∼20 years and should cause slow RV changes.

HIP 39681 (HD 66948, G5IV, 68 pc) is a single-lined binary with a long 4.7-yr period. Astrometric orbit with similar period has been published by Goldin & Makarov (2007). The large minimum secondary mass, 0.5 $\mathcal{M}_{\odot}$, indicates that the RV amplitude could be reduced by line blending.

HIP 40253 (HD 68119, F5, 116 pc) is a single-lined binary with P = 808 d, as well as an astrometric binary.

HIP 40724 (BD−14 2469, K5V, 35 pc) has only two RV measurements that differ by 2 km s^{-1}; it is an astrometric binary.

HD 71028 is a distant (480 pc) chromospherically active K0III giant for which we determine an orbit with P = 1130 d.

HIP 42507 (BD−05 2603, K6V, 26 pc) has a large $\chi^2/(N-1)$ caused by one outlying measurement, hence the RV variability is not certain.

HIP 42550 (HD 73394) is a distant (600 pc) G5III giant. Its visual companion B (ES 209) at 57″ separation is optical, with different PM and RV. Both stars were observed here, and we found that B has double lines. No orbit can be derived from our five spectra.

HIP 43820 (HD 75632, M1V, 11.6 pc) is a visual binary on a 609-yr orbit, currently at 3″ separation. The RV of the brighter component A varies slowly over the 14 years of our monitoring, while its mean value differs slightly from the two RVs of the component B. We therefore believe that it could be a triple system. Halbwachs et al. (2018) published nine pairs of RVs, splitting the CORAVEL correlation dips in two components. Combining these data with our RVs and with two RVs from Tokovinin & Smekhov (2002), we can fit an orbit with P = 1050 d, K_1 = 2.8 km s^{-1}, K_2 = 7.0 km s^{-1}, and γ = 44.6 km s^{-1}. The minimum masses are suspiciously small, 0.05 and 0.02 $\mathcal{M}_{\odot}$, and therefore we prefer not to publish this orbit.

HIP 46383 (BD+40 2208, K4V, 32 pc) is a double-lined pair with P = 8.5 d and equal components, q = 0.99. After the orbit was computed from our 12 RVs, the paper by Halbwachs et al. (2018) came to our attention. Here we fit the orbit to the combined set of 33 RVs. The small residuals of 0.38 and 0.43 km s^{-1} for the primary and secondary components, respectively, demonstrate the good quality of our RVs and the lack of substantial zero-point differences between the CORAVELs at Moletai and OHP and the VUES. Considering the physical companion at 56″(LEP 36), this is a triple system.

BD−08 2689 (M0V) shows an increasing RV over the 6 years of our monitoring. Simbad quotes only a crude parallax of 9.2±15.0 mas that places the star at 3 mag above the main sequence (see Fig. 1). This parallax is most likely inaccurate. *Gaia* DR2 provides no parallax because the star is a resolved 0″.2 binary BEU 13 with an estimated period of ∼80 yr.

HIP 46926 (BD+16 1992, G0, 107 pc) is a triple system. The outer 33″ pair is physical (common PM and parallax). We discovered the double-lined inner subsystem Aa,Ab with P = 3.1 days and determined its orbit. Comparison of the RV amplitudes with the estimated masses implies a low orbital inclination of 15°.

HIP 47133 (M0V) is the secondary component B of a young multiple system belonging to the β Pictoris moving group (Alonso-Floriano et al. 2015). The primary is HIP 47110 (HD 82939, G5V, 39 pc), at 162″separation from B. The two stars have common PM, RV, and parallax; the estimated period of A,B is ∼160 kyr. The component B was found to be a double-lined spectroscopic binary by Schlieder et al. (2012), but they have not provided its orbit. We observed the component B for almost 16 years and derive here an orbit with P = 4.39 days. The residuals are quite large, 2.7 km s^{-1}, partly because the star is faint and partly because of its chromospheric activity. The outstanding feature of this orbit is its large eccentricity of 0.47. This pair is still in the phase of tidal orbit circularization. However, more observations are needed to confirm and improve the orbit.

HIP 47899 (MCC 554, K4V, 79 pc) is also a double-lined binary with a period of 146 days and a small but statistically significant orbital eccentricity. The mass ratio is q = 0.94.

HIP 48346 (BD+38 2075, K8, 52 pc) is a double-lined binary with P = 79 d, rather large eccentricity e = 0.7, and no other known visual companions.

HIP 50156 (DK Leo, M0.7V, 23 pc) is a triple system composed of the 0″.1 visual binary A,B with an estimated period of ∼3 yr, also detected by astrometric acceleration, and the 73-day single-lined inner pair Aa,Ab found here. It is a variable star of BY Dra type. The system belongs to the β Pictoris group according to several authors such as (Schlieder et al. 2012; Alonso-Floriano et al. 2015; Messina et al. 2017) and has an extensive bibliography.

HIP 50271 (BD+26 2062, G0, 173 pc) is a distant (869″) optical companion to the nearby (37 pc) G0V star HIP 50355. Our observations lead to the single-lined orbit with P = 47.5 days.

HIP 52021 (BD−05 3108, K8, 38 pc) has a variable RV, but our data do not suffice to find its orbit.

HIP 54002 (AB Crt, K3V, 31 pc) is a BY Dra-type variable star with variable RV, but no known spectroscopic orbit.

HIP 54094 (BD+54 1411, unknown spectral type, 47 pc) has the first deviant RV measurement which suggests its variability. Further monitoring is needed.

HIP 56229 (BD+41 2201, M0, 44 pc) is a double-lined binary. The 186-day spectroscopic orbit derived here from only seven RVs is not very secure. The star is an X-ray source. Astrometric acceleration was detected.

HIP 57058 (GJ 435.1, K4V, 31 pc) is a spectroscopic and acceleration binary for which we derive a preliminary single-lined orbit with $P = 726$ d by combining our RVs with those of Halbwachs et al. (2018). These authors found that the correlation dips are double and measured the RVs of the secondary component. The VUES profiles are double as well. We also measure the RVs of both components. This means that the CORAVEL RVs derived by fitting a single component are biased both in our data and in those of Halbwachs et al. when the RV difference is small. We use CORAVEL RVs with a low weight and disregard some of them. The period and estimated masses of 0.69 $\mathcal{M}_{\odot}$ correspond to a semimajor axis of 57 mas. This star was resolved twice in 2018 by speckle interferometry at the Southern Astrophysical Research Telescope, SOAR, at similar separations and shows a fast orbital motion, in qualitative agreement with the two-year period (Tokovinin et al. 2019, in preparation).

The RVs of the secondary component do not vary in antiphase with the primary and therefore cannot be used to derive a double-lined orbit. Hypothetically, this is a triple system where the outer orbit has a small inclination (hence small K_1) and its secondary component contains a short-period subsystem. Spectroscopic monitoring with higher resolution and future astrometric orbits from *Gaia* and SOAR will clarify the architecture of this low-mass system.

BD+44 2120 (F5, 345 pc) is a distant triple system. The outer 6″.8 pair ES 123 is physical, based on the common distances and RVs (the PMs are very small). Its secondary component B is a single-lined binary with $P = 2.2$ days. We also observed the component C at 42″ separation. Its RV, as well as PM, are distinct, therefore the star C is unrelated (optical).

GQ Leo (TYC 870-798-1, K5Ve, 61 pc) has a slowly variable RV. Its mean value of −12.8 km s^{-1} differs from -15.7 ± 1.8 km s^{-1} measured by *Gaia* and from three RVs around −11 km s^{-1} reported by Griffin (2005). An orbit with $P \approx 572$ d and $K_1 = 2.8$ km s^{-1} can be fitted to all RVs. However, alternative periods are not excluded, and therefore we refrain from publishing this tentative orbit. The object is a 0″.25 pair MET 57Aa,Ab with an estimated period of ~45 years,. Some RV variation could therefore be caused by this binary. The WDS lists another companion at 9″.5, which is optical according to the *Gaia* astrometry.

HIP 57857 (G148-14, K0V, 54 pc) has a variable RV, but our data are not sufficient for the determination of its orbit. Astrometric acceleration is evident from comparison of the average PM of (−339.3, −44.4) mas yr^{-1} deduced from the difference of *Hipparcos* and *Gaia* positions with the "instantaneous" PM measured by *Gaia*: $\Delta\mu = (+18.2, -6.1)$ mas yr^{-1}. The 4″.3 pair LEP 46 is physical according to *Gaia* PM and parallax, meaning that this is a triple system. The component B has an RV of -14.3 ± 3.3 km s^{-1} (Gaia) and its PM matches the average PM of A.

HIP 57949 (MCC 622, M0.5Ve, 31 pc) also has a variable RV, likely with a long period.

HIP 59000 (HD 105065, K5V, 23 pc) is a triple or quadruple system. The outer 183″ binary (estimated period ~300 kyr) is physical. The main star is an acceleration binary. Our single RV measurement, −8.2 km s^{-1} , differs from the *Gaia* RV of -29.2 ± 13.6 km s^{-1} . The large error of the latter also signals variability. Two mutually discordant RVs were measured by Maldonado et al. (2010). It is not clear whether the spectroscopic and astrometric subsystems are the same or distinct.

HIP 60433 (BD+21 2415, K4V, 40 pc) and **HIP 60448** (MCC 654, K5V, 30 pc) both have variable RVs, but no orbits have been computed. The first is also an acceleration binary. Eighteen years of RV coverage is available for both stars.

HIP 61436 (GJ 9412, K5V, 30 pc) is a double-lined binary with $P = 299$ d.

HIP 62505 (HD 111312, K2V, 26 pc) is a close visual and spectroscopic binary WSI 74 with a period of 2.66 yr. Its combined orbit was determined by Tokovinin (2017). Another visual companion at 2″.7 was measured by *Hipparcos*, but never confirmed; it is not spotted by *Gaia* and therefore remains questionable.

HIP 62755 was originally mis-identified with a nearby K6V dwarf MCC 679. The *Gaia* parallax of 0.81 ± 0.03 mas places HIP 62755 among giants. We determined an orbit with $P = 6.12$ years from 11 RVs covering a time period 8.2 years.

HIP 63253 (GJ 490, M0V, 21 pc) has an RV trend, and therefore the period is longer than 7 years. This is a 2+2 quadruple system. The outer 16″ pair has a period of ~6 kyr. Both components were resolved into 0″.1 pairs with estimated periods of a few years. The observed RV variation is most likely related to the subsystem Aa,Ab.

HIP 63816 (GJ 497, M0V, 16 pc) is a 1″.6 visual binary WOR 23. We find its RV to be constant over a time span of 7 years.

HIP 63942 (BD+21 2486, K4V, 19 pc) has a constant RV. This is a visual binary HU 739 with an orbital period of 431 years and a semimajor axis of 2″.65.

HIP 65012 (GJ 507B, M3V, 14 pc) is the secondary component B of HIP 65011 (at 17″.8 distance) which itself is a visual and spectroscopic pair with $P = 200$ d. We measured RV(B) once and found −5.2 km s^{-1} ; *Gaia* measured it at -9.1 ± 0.6 km s^{-1} .

HIP 65026 (HD 115953, K0, 9 pc) is a remarkable triple system. The outer 1″.5 binary HU 644 has a good-quality visual orbit with a period of 49 yr. The inner subsystem Aa,Ab is also resolved as CHR 193 at 0″.1. Here we determined its single-lined orbit with a period of 447 d. A preliminary period of 450 d was announced by Beuzit et al. (2014). A preliminary combined orbit of the inner subsystem shows that the mutual inclination in this triple system is small.

HIP 65327 (HD 238224, K5V, 24 pc) was resolved by *Hipparcos* at 0″.3 separation and $\Delta m = 2.3$ mag. We computed its single-lined orbit with $P = 12.4$ years. However, the RV amplitude is likely reduced by line blending. A combined visual/spectroscopic orbit can be computed now. The WDS also mentions the wide CPM pair SHY 67 with a separation of 9°.4, too wide to be a bound binary.

GJ 513 (M3V, 19 pc) has a slowly variable RV.

HIP 65887 (HD 117466, K0, 3 kpc) is a distant giant for which we provide a single-lined orbit with a 3.3-year period. Its semimajor axis should be 11 mas, and, indeed, the astrometric acceleration was detected by *Hipparcos*.

HIP 66290 (HD 118244, F5V, 38 pc) is a single-lined binary with a period of 5.4 years, as well as acceleration binary. The orbit is determined from 36 RVs measured during 23 years.

HIP 67086 (K5, 46 pc) is a 0.″6 binary resolved by *Hipparcos* (estimated period ∼100 yr) containing a spectroscopic subsystem. We measured RVs of both components with VUES and determined the orbit of the secondary subsystem Ba,Bb with $P = 41$ d.

BD+26 2498 is a G5 giant with a DR2 parallax of 1.40±0.03 mas. Our 31 RVs measured over 18 years securely define the spectroscopic orbit with a period of 4.2 years. This orbit corresponds to the minimum secondary mass of 1 $\mathcal{M}_\odot$. The secondary component could be a compact remnant. *Gaia* is expected to detect acceleration or deliver a full astrometric orbit.

HIP 67808 (BD+13 2721, K7V, 22 pc) is a 0.″2 visual (and acceleration) binary with an estimated period of ∼10 years discovered by Beuzit et al. (2014). Our six RVs measured over 7 years are probably constant, with one measurement deviating from the rest.

BD+19 2735 (K2, 37 pc) is a single-lined binary with a period of almost 10 years; 1.5 orbital cycles of its eccentric orbit are covered. Rotational modulation was measured by Kiraga (2012).

HIP 68801 (HD 123034, G5, 51 pc) is a double-lined binary with a circular 2.8-day orbit and a mass ratio $q = 0.98$ (a twin). Nordström et al. (2004) discovered the RV variability but provided no orbit.

HIP 69549 (HD 124605, G0, 85 pc) is a double-lined pair with $P = 6$ d and nearly equal components, $q = 0.98$. The interferometric 0.″08 pair TOK 723 with $\Delta I = 2.4$ mag remains unconfirmed and could be spurious; its parameters are similar to the optical ghosts reported in the discovery paper by Tokovinin et al. (2018). If it were a triple system, the outer period would be around ∼10 yr. However, we do not see any modulation of the center-of-mass velocity over the 19 years covered by our data.

HIP 72508 (HR 5537, F5IV, 52 pc) has double lines but the period remains unknown. The WDS companion B at 15″ is optical according to its *Gaia* astrometry. However, *Gaia* detected another faint ($G = 17.42$ mag) star at 9.″2 separation with similar parallax and PM, therefore this system is at least triple.

BD+49 2364 is a giant according to the *Gaia* parallax of 0.97 ± 0.03 mas. Its RV shows a trend and has changed by 5 km s^{-1} . The orbital period is longer than 29.5 years covered by our data.

HIP 76941 (MCC 316, K5V, 50 pc) is a single-lined binary with $P = 267$ d.

HIP 77141 (BD+36 2641, K4/5V, 54 pc) has a well-defined orbit with $P = 17.3$ d and a very large (for this period) eccentricity of 0.84 ± 0.15. Better coverage near periastron of this orbit is needed to constrain the eccentricity.

HIP 78158 (K5V, 52 pc) is a triple system that consists of the wide 187″ physical pair A,B (LDS 983) and the single-lined spectroscopic subsystem Aa,Ab discovered here. Its orbital period is 322 d. We noted secondary dips in some spectra, but their RVs do not match the orbit.

HIP 79796 (BD+55 1823, CR Dra, M5.6V, 20 pc) is a low-mass flare star and an interferometric binary BLA 3, for which an orbit with a period of 4.04 yr was computed by Tamazian et al. (2008). We see double lines, but their RVs do not match the visual orbit. A tentative RV curve with a period of 1.57 yr is plotted in Fig. 5. Shkolnik et al. (2010) obtained two double-lined spectra and determined that the period is less than 530 d. More work is needed to reconcile RVs with position measurements and hopefully to compute the combined orbit.

HIP 80751 (BD+24 3014, K5V, 32 pc) has a variable RV measured over 18 years. We determined a tentative orbit with $P = 14.4$ yr, but new measurements and a better coverage are needed for its confirmation. Astrometric acceleration was detected.

BD+52 1968 (K8, 44 pc) is a 5.″6 visual binary ES 968 (estimated period ∼3 kyr). The RV of the component A, measured 13 times with VUES, is certainly variable with a long period. The RV of B was measured on only one night and agrees with the mean RV of A.

HIP 82506 (HD 152342, F4III, 67 pc) has a variable RV, but not enough data are available for orbit calculation. Is is also an astrometric binary.

BD+61 1678C (GJ 685, M1V, 14 pc) is the distant (738″) component to the visual pair A,B (GJ 684, HIP 86036, G0V) which has a period of 76 yr and the corresponding single-lined spectroscopic orbit. We monitored RV of the component C and found it to be constant, agreeing with the RV of A. The same conclusion was reached by Tokovinin (1992).

HIP 90274 (HD 170527, K0, 175 pc) is a giant observed over 16 years. The spectrum has blended double lines, but no orbit is derived yet.

HIP 91043 (HD 171488, V889 Her, G2V, 35 pc) has a double-lined spectrum and no spectroscopic orbit despite our 39 observations, mostly with unresolved CORAVEL dips. Several faint companions are listed in the WDS, but none of those are confirmed as physical.

HIP 92952 (G 229-18, M0V, 46 pc) is a quadruple system. The outer pair A,B (GIC 154) has a separation of 119″ and an estimated period of ∼300 kyr. The component A is a 0.″4 visual binary Aa,Ab resolved by *Hipparcos* that has not been measured since; its estimated period is ∼70 years. We see double lines in the spectrum. Stationary lines correspond to the visual secondary Ab and the moving lines to the primary Aa, which is a spectroscopic binary Aa1,Aa2 with a period of 8 d. The eccentricity of the spectroscopic orbit is small, but statistically significant: $e = 0.044 \pm 0.007$. The RV of the star Ab is about −15 km s^{-1} . Its measurements are not accurate owing to blending with the lines of Aa1.

HIP 94557 (G 185-12, M4.5V, 18 pc) is the brighter component of the wide visual binary WDS J19147+1918 (LDS 2020, 41″). Our three RVs show variability. Shkolnik et al. (2012) measured a very different RV of −80.9 km s^{-1} , quoted in Simbad.

HIP 94622 (GJ 751, M0, 29 pc) has a variable RV, and some spectra have double lines. The RV variability was also noted by Tokovinin (1992). This is a *Hipparcos* binary with 0.″2 separation and an estimated period of ∼10 yr. It is not clear whether the visual and spectroscopic systems correspond to the same pair or this is a triple system.

BD+77 767 (K8, 41 pc) is a single-lined binary with $P = 17.3$ d.

HIP 99969 (BD+06 4489, K4V, 44 pc) has double lines, but we are not yet able to determine its orbit.

HIP 101941 (HD 196928, K4III, 380 pc) is a single-lined binary with $P = 2.8$ yr, as well as an astrometric binary.

HIP 102300 (M0Ve, 21 pc) has a variable RV. The period is longer than the 8 yr covered by our data.

HIP 102320 (HD 335007, K5, 42 pc) belongs to a triple system where the outer 4.″4 pair ES 366 has a period of the order of ∼2 kyr and $\Delta m = 3$ mag. The main component A is a double-lined twin binary with $P = 21$ d and equal components, $q = 0.97$. The orbital inclination of the spectroscopic pair is about 55°.

HIP 102718 (BD+04 4551, F7Vw, 103 pc) is the primary component of WDS J20488+0512, a 6.″6 pair. Its RV is likely constant.

HIP 103375 (HD 235405, G0, 132 pc) belongs to WDS J20566+5250 (ADS 14465, A 1437, separation 1''.3). Its RV is likely constant.

HIP 104994 (BD+28 4035, G5, 143 pc) is a triple-lined system. The outer 0''.19 binary was first resolved by *Hipparcos* and has not been measured since; its period is ∼100 yr. Stationary lines in the spectrum belong to the visual secondary B with RV of −54 km s^{-1} . The pair of moving lines corresponds to the subsystem Aa,Ab with P = 52 d and systemic velocity of −46.8 km s^{-1} . Its inclination is about 52°.

HIP 105504 (HD 358435, K7, 42 pc) definitely has a variable RV, but not enough data for an orbit. Its astrometric acceleration was detected.

BD+47 3439 (K0, 115 pc) is an evolved star in the visual triple system ADS 15052, with separations of 1''.1 and 0''.2. The spectra have double lines, but the spectroscopic orbit remains to be determined. Either there is an additional spectroscopic subsystem, or the inner binary is going through the periastron of its eccentric orbit (its estimated period is ~80 years). The fact that *Gaia* DR2 measured the parallax favors the latter scenario because partially resolved sources do not have parallaxes in DR2.

HIP 110291 (HD 212029, G0, 62 pc) is a single-lined binary with a period of 2.1 yr. A similar period was determined by D. Latham (2012, private communication), while two astrometric orbits with periods of 2.07 and 2.17 yr and large eccentricities were computed by Goldin & Makarov (2006). The WDS lists several optical companions.

HIP 110526 (GJ 826, M3.0V, 15 pc) has a constant RV over the 8 years of our monitoring. It is a visual binary WOR 11 with P = 130 yr and semimajor axis 1''.61.

HIP 110978 (HD 213054, K2III, 800 pc) may have a mild RV trend over 34 days. It has astrometric acceleration.

HIP 111685 (BD+38 4818, M0Ve, 24 pc) is the main component of the triple system. The faint (V = 21.2 mag) outer component C is at 33''.4 distance from the main star, with common PM and parallax. The inner pair A,B, first resolved by *Hipparcos*, has a well-defined visual orbit with P = 16 yr. We fitted our RVs and all available positional measurements to a combined orbit and provide its spectroscopic elements here.

HIP 111942 (GJ 870, K8V, 31 pc) is a single-lined binary with P = 375 days. The orbit derived from our 20 RVs is very similar to the orbit published independently by Halbwachs et al. (2018) and based on 25 CORAVEL RVs. Here we list orbital elements fitted to the combined data, with a global rms residual of 0.32 km s^{-1} .

HIP 112040 (BD+18 5029, M0V, 31 pc) has a variable RV with a period longer than 15 yr, as well as astrometric acceleration.

HIP 112268 (BD+16 4806, K6V, 50 pc) has a variable RV. We computed an uncertain orbit with P = 4.35 yr which is not publishable until better coverage is obtained.

HIP 112523 (MCC 851, K5V, 37 pc) has a preliminary orbit with P = 8.9 yr derived from 13 RVs spanning a period of 15 yr. The eccentricity was fixed in the orbit fitting. Astrometric acceleration was detected.

HIP 116003 (GJ 1284, M2Ve, 16 pc) is a flare star and an X-ray source. As our two RVs are very different from each other, this object must be a fast spectroscopic binary. A variable RV was noted by Gizis et al. (2002).

BD+66 1664 (G5, 90 pc) is a single-lined binary with a circular three-day orbit. Fast synchronous rotation is responsible for its high chromospheric activity.

HIP 118212 (GJ 913, K7V, 17 pc) is a single-lined binary with a period of 872 d (2.4 yr). It is also an acceleration binary and suspected nonsingle star in *Hipparcos*. One interferometric resolution at 62 mas with ΔI = 1.4 mag was reported by Balega et al. (2007). The astrometric orbit by Goldin & Makarov (2006) with P = 885 d and e = 0.56 is similar to our spectroscopic orbit. However, their revised parallax of 67 mas is not confirmed by *Gaia*.

4.4. The triple system HIP 13460

This star, also known as BD+60 585 and GJ 3185, is a K3V dwarf at 39 pc from the Sun. The spectrum is double-lined, and the period of 76 d is readily found. However, all 30 RVs cannot be fitted by the common elements, leaving residuals of 1.6 and 2.0 km s^{-1} for Aa and Ab, respectively. Individual fits to the RVs measured with CORAVEL and VUES are better, but result in slightly different elements.

All RVs can be better modeled by assuming that the pair Aa,Ab moves slowly on an outer orbit. Astrometric acceleration reported by Makarov & Kaplan (2005) and confirmed by *Gaia* supports the triple-star hypothesis. We fitted the long-period orbit with K_1 = 4 km s^{-1} using `orbit3.pro` (Fig. 6). The rms residuals to the triple-star solution are 0.88 km s^{-1} for Aa and 3.23 km s^{-1} for Ab. The component Ab may contain a short-period subsystem.

The masses of Aa and Ab estimated from the absolute magnitudes and the mass ratio are 0.78 and 0.71 $\mathcal{M}_\odot$. Comparison with the minimum masses leads to the inclination $i_{\rm Aa,Ab}$ = 32°. The minimum mass of the tertiary component B is 0.29 $\mathcal{M}_\odot$. Although the semimajor axis of the outer orbit computed from the period and mass sum is 92 mas, there is little hope of resolving A,B directly owing to the expected faintness of B. On the other hand, *Gaia* can provide astrometric orbits for both inner and outer systems. To do so, an initial guess of the orbital periods and other parameters will likely be needed, and our work provides these parameters. It is unlikely that *Gaia* astrometry of this complex system can be interpreted correctly from its pipeline alone, without additional inputs.

5. Summary

The main results of this work are as follows.

- A large set of RV measurements spanning three decades.
- Determination of 57 spectroscopic orbits, 53 of those for the first time.
- Discovery of 20 new nearby hierarchical systems.
- Discovery of interesting stellar systems. For example, in the young triple system HIP 47110, the inner orbit with P = 4.4 d and e = 0.47 is apparently still circularizing.

Most orbits presented here refer to nearby K- and M-type dwarfs and result from long-term RV monitoring. Our sample includes 857 stars from the McCormick catalog and 188 stars from the Gliese catalog. Observational data on this sample are given in Table 4 of Sperauskas et al. (2016). A total of 67 spectroscopic orbits are known for these stars, including 35 determined here. In addition, there are 70 stars with variable RVs without orbital elements identified from our data, from the literature (e.g. Halbwachs et al. 2018), or by comparing our RVs with those from *Gaia* DR2. The latter group contains 30 objects where the RV difference exceeds 2.5 km s^{-1} (3σ). For stars with constant RV, the mean RV difference between our CORAVEL and *Gaia* RVs is 0.21 km s^{-1} with the rms scatter of σ = 0.74 km s^{-1} . Figure 7 illustrates the contribution of this work to the census of spectroscopic binaries among K- and M-dwarfs.

We continue observations of the identified RV variables with the VUES spectrograph in order to detect double-lined spectroscopic binaries among them and to calculate their orbital parameters. Stars of this type may not be recognized by *Gaia* due to the relatively low resolution of its spectrometer.

Acknowledgements. It is a pleasure to thank an anonymous referee for careful reading and valuable comments. We used the Simbad service operated by the Centre des Données Stellaires (Strasbourg, France). This work also made use of data from the European Space Agency (ESA) mission *Gaia*[3], processed by the *Gaia* Data Processing and Analysis Consortium (DPAC, https://www.cosmos.esa.int/web/gaia/dpac/consortium). Funding for the DPAC has been provided by national institutions, in particular the institutions participating in the *Gaia* Multilateral Agreement.

References

Albareti, F. D., Allende Prieto, C., & Almeida, A. 2017, ApJS, 233, 48
Alonso-Floriano, F. J., Caballero, J. A., Cortès-Contreras, M., Solano, E., & Montes, D. 2015, A&A, 583, 85
Balega, I. I., Balega, Y. Y., Maksimov, A. F., et al. 2007, Astrophys. Bull., 62, 339
Baranne, A., Mayor, M., & Poncet, J. L. 1979, Vistas in Astron., 23, 279
Baroch, D., Morales, J. C., Ribas, I. et al. 2018, A&A, 619, 32
Beuzit, J.-L., Ségransan, D., Forveille, T., et al. 2014, A&A, 425, 997
Bressan, A., Marigo, P., Girardi, L., et al. 2012, MNRAS, 427, 127
Chanamé, J. & Ramirez, I. 2012, ApJ, 746, 102
Fekel, F. C. & Marschall, L. A. 1991, AJ, 102, 1439
Gaia Collaboration, Brown, A. G. A., Vallenari, A., Prusti, T., et al. 2018, A&A, 595, A1, (Vizier Catalog I/345/gaia2)
Gizis, J. E., Reid, I. N., & Hawley, S. L. 2002, AJ, 123, 3356
Gliese, W. & Jahreiß, H. 1991, The Astronomical Data Center CD-ROM: Selected Astronomical Catalogs, I
Goldin, A. & Makarov, V. V. 2006, ApJS, 166, 341
Goldin, A. & Makarov, V. V. 2007, ApJS, 173, 137
Griffin, R. F. 2005, Observatory, 125, 323
Halbwachs, J. L., Mayor, M., & Udry, S. 2018, A&A, 619, 81
Halbwachs, J. L., Mayor, M., Udry, S., & Arenou, F. 2003, A&A, 397, 159
Janson, M., Durkan, S., Hippler, S., et al. 2017, A&A, 599, 70
Jurgenson, C., Fischer, D., McCracken, T., et al. 2016, JAI, 5, 500033
Kiraga, M. 2012, Acta Astron., 62, 67
Latham, D. W., Stefanik, R. P., Torres, G., et al. 2002, AJ, 124, 1144
Makarov, V. V. & Kaplan, G. H. 2005, AJ, 129, 2420
Maldonado, J., Martinez-Arnaiz, R. M., Eiroa, C., Montes, D., & Montesinos, B. 2010, A&A, 521, 12
Malkov, O. Y., Oblak, E., Snegireva, E. A., & Torra, J. 2006, A&A, 446, 785
Mason, B. D., Wycoff, G. L., Hartkopf, W. I., Douglass, G. G., & Worley, C. E. 2001, AJ, 122, 3466, (WDS)
Messina, S., Lanzafam, A. C., Malo, L., et al. 2017, A&A, 607, 3
Moe, M., Kratte, K. M., & Badenes, C. 2018, ArXiv e-prints [arXiv:1808.02116]
Montes, D., González-Peinado, R., Tabernero, H. M. et al. 2018, MNRAS, 479, 1332
Niedever, D. L., Marcy, G. W., Butler, R. P., Debra, A., & Vogt, S. S. 2002, ApJS, 141, 503
Nordström, B., Mayor, M., Andersen, J., et al. 2004, A&A, 418, 989
Schlieder, J. E., Lépine, S., & Simon, M. 2012, AJ, 144, 109
Shkolnik, E. L., Anglada-Escude, G., Liu, M., et al. 2012, ApJ, 758, 56
Shkolnik, E. L., Hebb, L., Liu, M., Reid, I. N., & Collier, C. A. 2010, ApJ, 716, 1522
Sperauskas, J., Bartašiute, S., Boyle, R. P., et al. 2016, A&A, 596, 116
Steinmetz, M., Zwitter, T., Siebert, A., et al. 2006, AJ, 132, 1645
Tamazian, V. S., Docobo, J. A., Balega, Y. Y., et al. 2008, AJ, 136, 974
Tokovinin, A. 2018, ApJS, 235, 6
Tokovinin, A. & Latham, D. W. 2017, ApJ, 838, 54
Tokovinin, A., Mason, B. D., Hartkopf, W. I., Mendez, R. A., & Horch, E. 2018, AJ, 155, 235
Tokovinin, A. A. 1992, A&A, 256, 121
Tokovinin, A. A. 2014, AJ, 147, 87
Tokovinin, A. A. 2017, AJ, 154, 110
Tokovinin, A. A. & Smekhov, M. G. 2002, A&A, 382, 118
Upgren, A. R. & Weis, E. W. 1989, in Star Catalogues: A Centennial Tribute to A. N. Vyssotsky, eds. A. G. D. Philip, & A. R. Upgren, 19
Zhao, G., Zhao, Y.-H., Chu, Y.-Q., Jing, Y.-P., & Deng, L.-C. 2012, RAA, 12, 723

[3] https://www.cosmos.esa.int/gaia

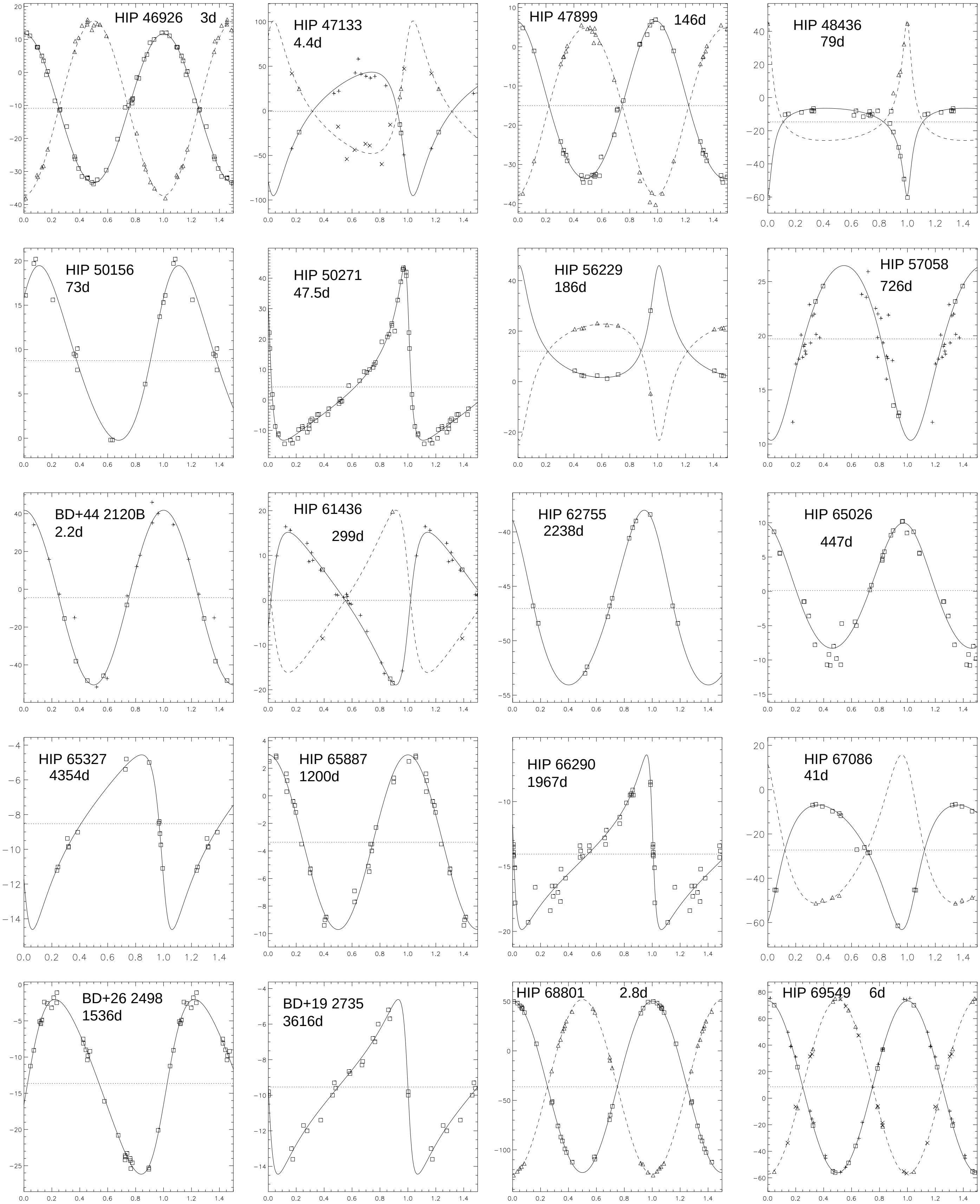

Fig. 4. RV curves (continued).

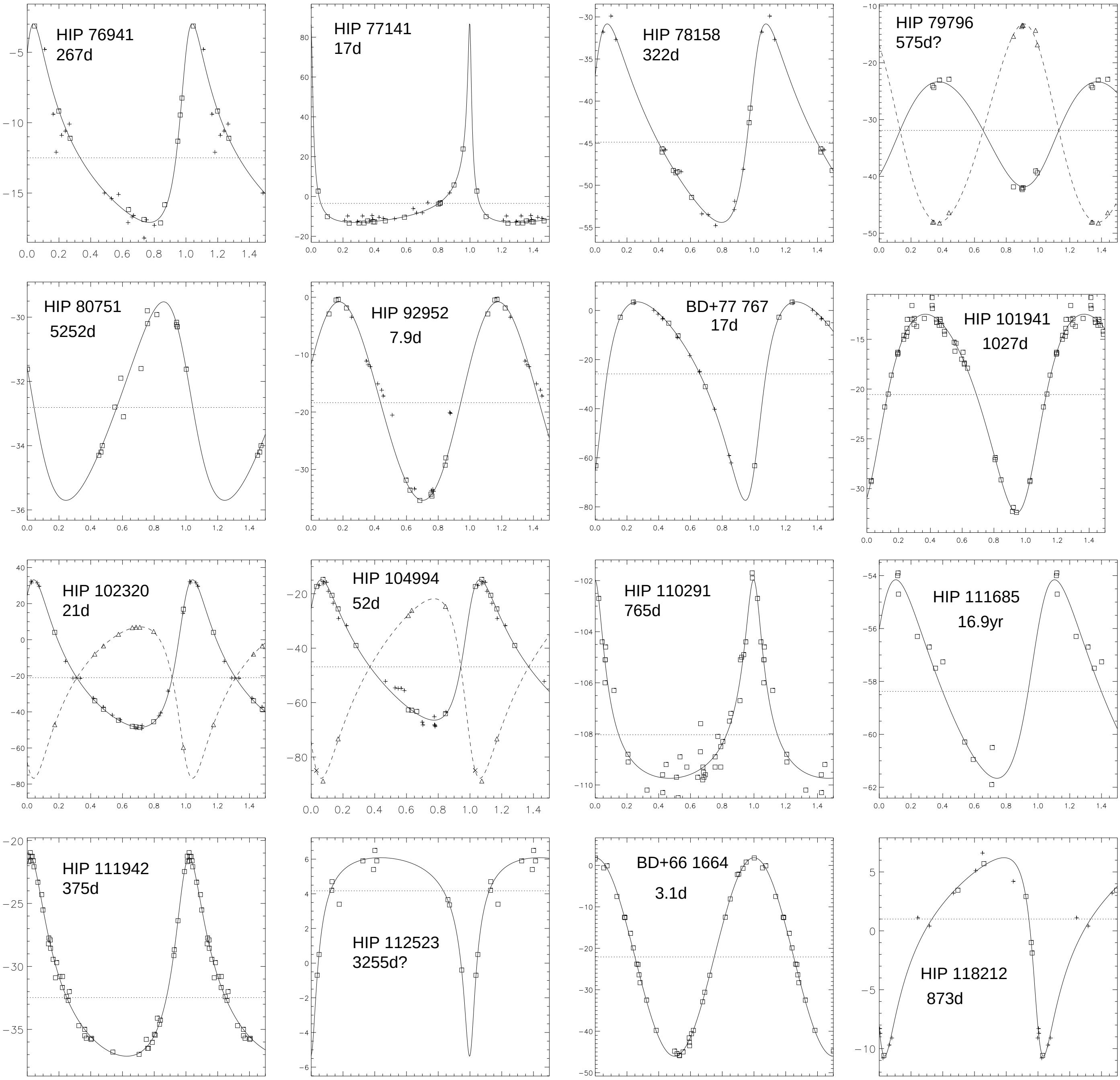

Fig. 5. RV curves (continued).

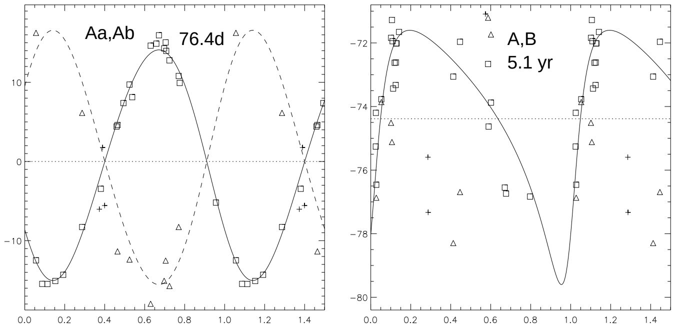

Fig. 6. RV curves of HIP 13460. Left: Inner subsystem, P = 76.4 d. Right: Outer subsystem, P = 5.1 yr. Radial velocities derived from blended dips are plotted as crosses and are given small weights in the orbit fit.

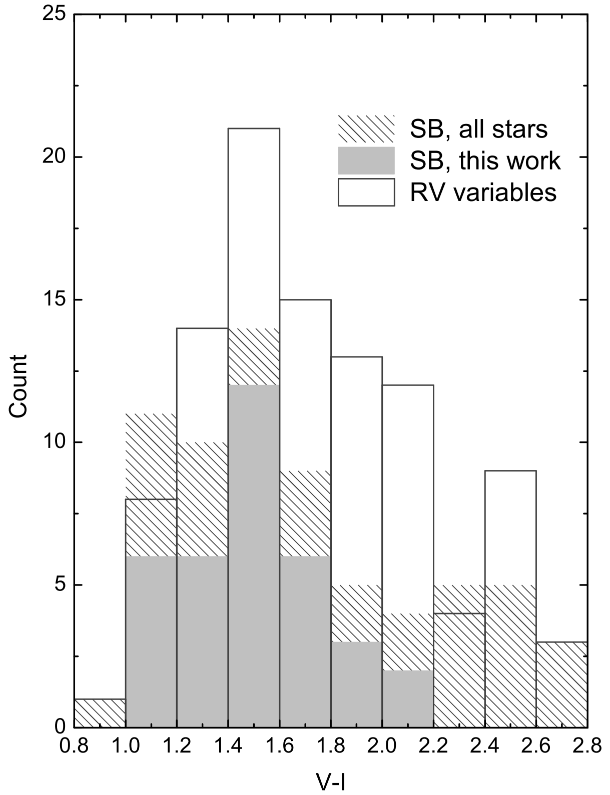

Fig. 7. Histogram of the number of spectroscopic binaries and stars with variable RVs in the sample of K- and M-dwarfs of Sperauskas et al. (2016).

Table 1. Object list

Name	RA	Dec	V	ϖ	Sp.	Type	N	ΔT	$\langle$RV$\rangle$	rms	$\chi^2/(N-1)$
	J2000		(mag)	(mas)	type			(d)	(km s^{-1})	(km s^{-1})	
HIP 96	00 01 13.19	+13 58 30.3	10.59	23.25	M0.5	V	7	2555	−7.93	1.49	23.6
BD+13 5195B	00 01 12.87	+13 58 19.7	11.12	27.77	M1	V	5	2541	−10.15	0.82	10.4
HIP 374	00 04 40.08	+34 15 54.4	7.08	5.64	K0	C	4	6231	−24.02	0.35	1.8
HIP 375	00 04 40.19	+34 16 19.8	10.13	1.00	–	C	4	6242	−9.17	0.24	0.9
BD+33 4827D	00 04 33.54	+34 15 03.5	10.55	4.56	F9	S1	49	6242	−23.48	...	...
HIP 1412	00 17 40.90	−08 40 56.2	10.95	31.57	K7V	V	6	1479	15.73	14.41	99.0
HIP 3428	00 43 41.42	+23 53 07.1	10.97	22.18	K7	S2	16	2168	−6.65	...	...
HIP 5110	01 05 29.92	+15 23 24.2	9.17	36.65	K3.5V	C	4	2915	−5.72	0.35	2.4
HD 6440B	01 05 29.76	+15 23 15.5	9.93	37.41	K8V	V	8	2915	−3.22	1.23	12.7
HD 8691	01 26 09.28	+31 54 52.6	9.24	19.96	G0	S1	42	5440	−36.18	...	...
HIP 9867	02 06 57.21	+45 11 04.1	10.24	51.47	M0V	S2	17	5479	61.42	...	...
HIP 10258	02 11 57.98	+04 21 41.8	9.72	21.36	K5	S2	30	4742	−59.15	...	...
BD+49 646	02 22 33.89	+50 33 36.9	9.65	18.91	–	s2	8	4711	−10.00	...	...
HIP 11437	02 27 29.25	+30 58 24.6	10.12	24.36	K7V	C	10	5884	5.98	0.46	1.8
HIP 12787	02 44 21.36	+10 57 41.3	11.10	20.51	M0Ve	s2	12	2970	4.20	...	...
HIP 13398	02 52 25.03	+26 58 29.9	11.05	42.67	M2V	V?	13	5459	−11.59	0.74	3.7
HIP 13460	02 53 18.50	+60 51 11.7	9.20	25.75	K3V	S2	30	2965	−73.61	...	...
HIP 14478	03 06 51.34	+40 21 33.5	9.63	37.02	K6	S1	15	2917	−50.87	...	...
HIP 14669	03 09 30.79	+45 43 57.9	10.17	57.11	M2V	V	9	2629	−4.51	1.99	35.2
HIP 14864	03 11 56.83	+61 31 13.0	10.05	39.82	M0Ve	S2	33	3023	−32.10	...	...
BD+03 480	03 28 14.92	+04 09 47.4	9.49	11.99	G0	C	11	4764	12.66	0.57	1.1
HIP 17102	03 39 48.96	+33 28 24.3	9.05	25.49	K2	S2	23	2777	4.27	...	...
GJ 3248	03 48 38.24	+73 32 35.3	11.32	62.71	M1V	V?	11	2971	−8.08	0.78	5.0
HIP 18448	03 56 36.22	+69 50 55.9	9.33	6.71	K0	S1	29	6014	16.66	...	...
HIP 19410	04 09 26.37	−14 41 54.1	10.61	24.67	K5V	V	3	4350	6.34	7.97	99.0
HIP 19915	04 16 19.83	+36 44 02.8	8.98	6.01	F8	S2	41	10496	−8.16	...	...
HD 279846	04 26 09.68	+34 09 34.2	10.50	12.14	K2	S2	28	6089	12.43	...	...
HIP 20709	04 26 15.05	+34 42 57.2	8.29	7.60	F5	S2	27	4743	44.76	...	...
HIP 21710	04 39 42.61	+09 52 19.5	9.19	36.80	K2	S1	16	1340	−25.93	...	...
HIP 21845	04 41 47.25	+28 39 35.9	8.85	8.70	F8	V?	11	5191	11.20	0.59	2.3
HIP 23550	05 03 51.96	+24 58 22.1	7.43	13.69	G8V	V	16	3271	54.18	1.18	10.6
HIP 24488	05 15 15.46	+47 10 14.6	6.92	8.73	G5III	s2	10	7146	24.42	...	...
GJ 220	05 53 14.04	+24 15 32.9	10.82	51.50	M2.0V	V	13	6089	26.45	1.75	28.2
HIP 28663	06 03 08.64	+14 21 54.4	8.31	9.74	F4IV	S1	30	1722	−25.10	...	...
HIP 29295	06 10 34.62	−21 51 52.7	8.12	173.70	M1V	C	6	5754	4.71	0.32	0.3
HIP 29316	06 10 54.80	+10 19 05.0	10.39	91.65	M2.5V	V	10	2567	52.81	1.27	15.4
HIP 30269	06 22 02.50	−05 27 17.0	8.06	3.22	F5V	V	14	5389	20.29	14.85	99.0
HIP 33560	06 58 26.05	−12 59 30.6	9.16	44.41	K4V	V?	14	8376	−4.33	0.96	2.3
HIP 34341	07 07 09.31	+03 26 50.7	9.87	38.26	K5	S1	21	5703	−17.35	...	...
HIP 35706	07 22 02.05	+68 16 27.6	10.10	23.84	K5V	S1	21	5824	−29.95	...	...
HIP 36758	07 33 34.77	+39 27 14.0	9.75	5.95	F8	V?	11	1540	36.73	1.02	2.7
HIP 38195	07 49 32.01	+41 28 08.3	9.41	8.98	G5	C?	10	6508	71.24	1.69	7.1
HIP 39681	08 06 34.41	+22 27 24.2	7.22	14.73	G5IV	S1	68	10984	−0.57	...	...
HIP 40253	08 13 17.31	+49 13 15.5	8.54	8.59	F5	S1	67	6961	−3.26	...	...
HIP 40724	08 18 44.42	−15 12 08.5	9.87	28.85	K5V	V	2	797	88.15	1.05	7.6
HD 71028	08 26 07.19	+28 24 10.7	8.01	2.21	K0III	S1	29	7645	34.15	...	...
HIP 42507	08 40 00.27	−06 28 33.1	9.88	38.80	K6V	C?	5	2245	−12.14	1.38	17.1
HIP 42550	08 40 22.54	+51 45 06.6	7.70	1.70	G5III	C	11	10684	−101.16	0.44	1.3
HD 73394B	08 40 18.25	+51 45 46.8	11.54	1.41	–	s2	5	4133	−32.54	...	...
HIP 43820	08 55 24.82	+70 47 39.2	8.61	86.32	M1V	V	19	5226	44.64	...	...
HD 75632B	08 55 24.82	+70 47 39.2	8.86	86.32	M1V	C	2	326	43.81	0.08	0.3
HIP 46383	09 27 28.37	+39 30 17.9	9.85	30.60	K4V	S2	12	2585	−32.36	...	...
BD-08 2689	09 28 51.52	−09 16 00.8	10.54	9.20	M0V	V	4	2208	−14.81	1.55	24.5
HIP 46926	09 33 52.46	+15 29 31.2	9.47	9.32	G0	S2	38	5046	−10.86	...	...
HIP 47133	09 36 15.91	+37 31 45.5	11.02	25.78	M0V	S2	16	5819	−0.68	...	...
HIP 47899	09 45 44.26	+50 14 08.3	11.19	12.58	K4V	S2	30	6588	−15.01	...	...
HIP 48346	09 51 18.98	+37 36 15.9	9.96	19.28	K8	S2	23	2828	−14.65	...	...
HIP 50156	10 14 19.18	+21 04 29.6	10.08	42.74	M0.7V	S1	13	2527	8.74	...	...
HIP 50271	10 15 52.67	+25 50 01.2	9.44	5.77	G0	S1	49	10619	4.29	...	...

Table 1. continued.

Name	RA	Dec	V	ϖ	Sp.	Type	N	ΔT	$\langle$RV$\rangle$	rms	$\chi^2/(N-1)$
	J2000		(mag)	(mas)	type			(d)	(km s^{-1})	(km s^{-1})	
HIP 52021	10 37 47.41	−06 23 22.5	9.94	26.41	K8	V	8	6592	−11.58	7.11	99.0
HIP 54002	11 02 50.12	−09 19 49.3	9.04	32.07	K3V	V	6	6554	−6.78	0.98	9.4
HIP 54094	11 04 07.16	+53 22 55.5	9.98	21.45	?	V?	9	6554	−23.88	0.58	4.2
HIP 56229	11 31 36.39	+40 30 01.2	9.75	22.85	M0	S2	8	473	12.02	…	…
HIP 57058	11 41 49.59	+05 08 26.5	9.59	32.26	K4V	S1	11	2602	18.90	…	…
BD+44 2120A	11 43 48.16	+44 10 46.5	11.22	2.86	F5	C	5	4136	−5.73	0.74	3.6
BD+44 2120B	11 43 47.90	+44 10 40.3	11.45	3.06	?	S1	17	4136	−4.39	…	…
BD+44 2120C	11 43 44.06	+44 10 49.1	11.04	3.06	?	C	11	7654	15.01	0.57	0.6
GQ Leo	11 47 45.73	+12 54 03.4	10.83	16.29	K5Ve	C	12	5468	−12.77	1.31	15.0
HIP 57857	11 51 56.21	+33 07 11.4	10.97	18.50	K0V	V	11	6645	−20.28	2.96	95.6
HIP 57949	11 53 05.24	+18 55 48.1	11.73	32.00	M0.5V	V	7	5529	6.82	2.48	33.2
HIP 59000	12 05 50.66	−18 52 30.9	10.02	42.72	K5V	-	1	0	−8.20	…	…
HIP 60433	12 23 26.85	+20 17 27.0	10.02	24.99	K4V	V	15	6594	−40.01	6.20	99.0
HIP 60448	12 23 34.71	+27 54 47.6	11.41	33.82	K5V	V	5	6592	−31.14	1.39	22.8
HIP 61436	12 35 19.72	+34 04 06.6	10.51	24.43	K5V	S2	24	2671	−0.01	…	…
HIP 62505	12 48 32.31	−15 43 10.1	7.89	39.21	K2.5V	V	12	4417	−1.87	3.35	32.9
HIP 62755	12 51 34.58	+59 50 25.9	11.31	0.81	K?	S1	11	3000	−47.03	…	…
HIP 63253	12 57 40.21	+35 13 30.1	10.68	46.84	M0V	V	11	2615	−10.00	1.32	25.7
HIP 63816	13 04 46.60	+55 54 10.1	10.75	30.63	M0V	C	3	2598	−22.47	0.32	1.6
HIP 63942	13 06 15.40	+20 43 45.3	9.40	53.18	K4V	C	13	5545	−2.84	0.57	1.3
HIP 65012	13 19 34.69	+35 06 24.5	11.90	73.99	M3V	-	1	0	−5.20	…	…
HIP 65026	13 19 45.65	+47 46 41.0	8.76	109.98	M2V	S2	27	2629	0.12	…	…
HIP 65327	13 23 23.30	+57 54 22.1	9.56	41.47	K5V	S1	15	6115	−8.53	…	…
GJ 513	13 29 21.31	+11 26 26.5	11.92	52.30	M3V	V	4	416	29.55	2.73	8.5
HIP 65887	13 30 22.60	+07 24 54.5	7.63	3.29	K0	S1	25	3674	−3.42	…	…
HIP 66290	13 35 11.42	+22 29 59.0	6.99	26.29	F5V	S1	36	8395	−14.04	…	…
HIP 67086	13 45 02.39	+02 05 31.5	10.78	21.67	K5	C?	14	2886	−27.23	…	…
BD+26 2498	13 49 18.69	+25 52 54.2	9.85	1.40	G5	S1	31	6654	−13.64	…	…
HIP 67808	13 53 27.56	+12 56 33.4	9.77	45.62	K7V	V?	6	2659	−18.71	0.43	2.2
BD+19 2735	13 58 13.62	+19 17 11.8	9.31	27.17	K2	S1	20	5133	−9.53	…	…
HIP 68801	14 05 03.72	+10 00 48.9	8.68	19.58	G5	S2	24	5429	−36.32	…	…
HIP 69549	14 14 12.16	+18 05 06.8	7.98	11.72	G	S2	29	6951	8.58	…	…
HIP 71904	14 42 26.26	+19 30 12.7	10.03	42.24	K5V	C	2	2550	−28.08	0.09	0.2
HIP 71914	14 42 33.81	+19 28 48.6	9.12	41.70	K5V	-	1	0	−28.70	…	…
HIP 72508	14 49 32.38	+51 22 28.2	6.48	19.09	F5IV	s2	11	7052	−6.13	…	…
BD+49 2364	15 13 25.00	+49 00 24.0	10.77	0.97	?	V	22	10789	−74.33	1.69	19.7
HIP 76941	15 42 38.57	+31 56 45.5	10.88	20.10	K5V	S1	26	2886	−12.50	…	…
HIP 77141	15 45 00.29	+35 57 40.9	10.11	18.50	K4/5V	S1	30	2913	−3.46	…	…
HIP 78158	15 57 33.88	+34 32 22.8	10.83	19.30	K5V	S1	19	2748	−44.84	…	…
HIP 79796	16 17 05.39	+55 16 09.1	9.46	49.35	M1.5V	S1	14	2895	−30.82	12.49	99.0
HIP 80751	16 29 14.36	+23 46 33.9	10.08	30.84	K5V	S1	14	6554	−32.81	…	…
BD+52 1968A	16 39 13.76	+52 37 39.4	10.01	22.86	K8	V	13	2926	−8.55	3.30	99.0
BD+52 1968B	16 39 13.10	+52 37 38.2	11.40	22.71	–	C	2	0	−8.69	0.39	6.9
HIP 82506	16 51 46.46	+25 24 00.7	7.09	14.84	F4III	V	8	4785	−25.39	4.76	99.0
BD+61 1678C	17 35 34.49	+61 40 53.6	9.97	69.83	M1V	C	9	3105	−15.33	0.75	2.1
HIP 86221	17 37 10.77	+27 53 47.2	9.20	32.00	M0V	C	2	2825	−42.55	0.33	3.3
BD+27 2853C	17 37 11.41	+27 53 51.4	11.61	31.09	K5	-	1	0	−43.39	…	…
HIP 90274	18 25 10.11	+64 50 18.3	6.86	5.70	K0	s2	28	5881	−52.07	…	…
HIP 91043	18 34 20.10	+18 41 24.2	7.45	28.27	G2V	s2	39	4879	−22.21	…	…
HIP 92952	18 56 15.93	+54 31 48.1	10.37	21.51	M0V	S1	27	2944	−18.38	…	…
HIP 94557	19 14 39.16	+19 19 03.7	11.54	55.24	M4.5V	V	3	2904	−4.28	19.34	99.0
HIP 94622	19 15 18.84	+24 53 49.5	9.78	34.57	M0	s2	7	2989	−72.83	…	…
BD+77 767	20 11 00.50	+77 43 18.4	10.30	24.54	K8	S1	18	2822	−25.83	…	…
HIP 99969	20 16 55.43	+06 55 18.3	9.47	22.67	K4V	s2	8	2611	−56.38	…	…
HIP 101941	20 39 29.75	+28 05 18.6	7.78	2.63	K4III	S1	46	4775	−20.56	…	…
HIP 102300	20 43 41.37	+64 16 54.1	11.38	46.53	M0Ve	V	5	2963	15.51	1.25	11.8
HIP 102320	20 43 53.36	+31 19 10.4	9.96	24.06	K5	S2	29	3013	−21.08	…	…
HIP 102718	20 48 50.72	+05 11 58.8	9.69	9.70	F7Vw	C?	6	4290	−117.67	0.64	2.8
HIP 103375	20 56 37.80	+52 49 36.9	9.66	7.55	G0	C?	11	4418	−47.55	0.53	2.5
HIP 104994	21 15 54.95	+28 57 47.4	10.41	6.97	G5	S3	30	6669	−46.87	…	…

Table 1. continued.

Name	RA	Dec	V	ϖ	Sp.	Type	N	ΔT	$\langle$RV$\rangle$	rms	$\chi^2/(N-1)$
	J2000		(mag)	(mas)	type			(d)	(km s^{-1})	(km s^{-1})	
HIP 105504	21 22 07.78	−10 30 47.9	10.33	24.00	K7	V	5	2613	7.40	17.45	99.0
BD+47 3439	21 30 48.00	+48 27 25.4	8.66	7.12	K0	s2	14	5465	10.04	…	…
HIP 110291	22 20 23.85	+46 25 05.7	8.51	16.12	G0	S1	40	1571	−108.04	…	…
HIP 110526	22 23 29.10	+32 27 33.9	10.76	64.47	M3.0V	C	13	2940	−19.90	0.52	2.4
HIP 110978	22 29 04.21	−13 42 01.8	9.17	1.25	K2III	V?	3	34	−1.37	0.82	6.3
HIP 111685	22 37 29.90	+39 22 51.6	9.41	41.99	M0Ve	S1	10	5457	−58.38	…	…
HIP 111942	22 40 30.30	+43 00 47.4	9.83	31.92	K8V	S1	20	2940	−31.76	…	…
HIP 112040	22 41 34.99	+18 49 27.5	10.51	31.85	M0V	V	13	5469	−15.94	1.17	10.9
HIP 112268	22 44 24.92	+17 33 23.8	10.19	19.83	K6V	V	13	5521	−38.11	0.95	8.7
HIP 112523	22 47 30.45	+19 13 27.4	10.29	26.95	K5V	S1	13	5458	3.97	1.86	28.7
HIP 116003	23 30 13.44	−20 23 27.5	11.11	62.67	M2Ve	V	2	7	−6.83	7.07	91.2
BD+66 1664	23 58 10.67	+67 33 59.7	8.73	11.13	G5	S1	33	1175	−22.08	…	…
HIP 118212	23 58 43.51	+46 43 44.9	9.62	58.41	K7V	S1	18	2986	1.00	…	…

Table 3. Spectroscopic orbits

Name	P	T	e	ω_A	K_1	K_2	γ	rms$_{1,2}$	$M_{1,2}\sin^3 i$
	(d)	(+24 00000)	(deg)	(km s^{-1})	(km s^{-1})	(km s^{-1})	(km s^{-1})		($\mathcal{M}_\odot$)
BD+33 4827D	67.9618	51794.504	0.197	280.4	10.263	…	−23.478	0.58	>0.2
	±0.0035	±0.633	±0.010	±3.6	±0.125	…	±0.080	…	…
HIP 3428	97.250	58183.305	0.391	21.6	25.244	26.490	−6.648	0.52	0.56
	±0.015	±0.266	±0.005	±1.1	±0.197	±0.211	±0.072	0.46	0.53
HD 8691	581.17	55965.5	0.544	313.5	2.366	…	−36.183	0.54	>0.08
	±1.21	±5.1	±0.036	±5.5	±0.110	…	±0.065	…	…
HIP 9867	897.0	56004.0	0.0	0.0	8.057	11.347	61.419	0.38	0.40
	±2.3	±5.8	fixed	fixed	±0.114	±0.184	±0.079	0.37	0.28
HIP 10258	5.88554	54206.1875	0.0	0.0	66.011	64.231	−59.148	0.92	0.66
	±0.00001	±0.0022	fixed	fixed	±0.176	±0.189	±0.085	0.88	0.68
HIP 13460 Aa,Ab	76.433	58410.20	0.057	124.1	14.565	16.060	…	0.88	0.12
	±0.014	±3.20	±0.016	±14.2	±0.254	±1.508	…	3.23	0.11
HIP 13460 AB	1862:	55433	0.502	232.8	4.00	…	−74.386	…	>0.29
	±25	±149	±0.186	±7.4	±2.04	…	±0.577	…	…
HIP 14478	1325.2	57011.8	0.369	142.4	5.814	…	−50.871	0.22	>0.34
	±7.8	±16.5	±0.033	±5.8	±0.162	…	±0.183	…	…
HIP 14864	59.428	56470.94	0.642	130.3	27.626	31.667	−31.907	0.37	0.33
	±0.005	±0.07	±0.006	±0.8	±0.256	±1.020	±0.138	1.15	0.29
HIP 17102	183.113	57305.62	0.6115	350.09	25.134	24.121	4.273	0.42	0.56
	±0.019	±0.17	±0.0020	±0.49	±0.124	±0.128	±0.073	0.41	0.58
HIP 18448	1538.9	54793.6	0.478	210.6	6.469	…	16.657	0.34	>0.38
	±2.6	±5.9	±0.018	±2.3	±0.117	…	±0.088	…	…
HIP 19915	7.30032	50087.8789	0.0	0.0	27.326	30.620	−8.157	1.25	0.078
	±0.00003	±0.0092	fixed	fixed	±0.160	±0.182	±0.107	1.44	0.069
HD 279846	15.4860	55271.598	0.039	245.1	44.723	47.041	12.429	0.78	0.63
	±0.0001	±0.189	±0.003	±4.5	±0.217	±0.225	±0.075	1.09	0.60
HIP 20709	140.748	56222.61	0.557	280.0	23.200	31.750	44.060	0.19	0.84
	±0.020	±0.34	±0.007	±0.6	±0.086	±0.332	±0.067	0.19	0.60
HIP 21710	610.43	56635.1	0.415	269.9	4.596	…	−27.124	0.75	>0.17
	±0.15	±4.2	±0.018	±3.4	±0.099	…	±0.067	…	…
HIP 28663	8.5542	52158.14	0.079	255.3	30.129	…	−25.105	0.68	>0.35
	±0.0001	±0.12	±0.006	±5.0	±0.229	…	±0.136	…	…
HIP 34341	875.37	55875.7	0.507	328.7	4.561	…	−17.353	0.45	>0.20
	±1.69	±8.6	±0.026	±5.4	±0.284	…	±0.106	…	…
HIP 35706	4741	56641	0.337	266.5	5.639	…	−29.953	0.22	>0.57
	±73	±41	±0.022	±4.6	±0.098	…	±0.125	…	…
HIP 39681	1717.7	51745.8	0.508	76.3	8.077	…	−0.569	0.47	>0.51
	±0.7	±3.7	±0.009	±1.5	±0.116	…	±0.054	…	…
HIP 40253	897.83	54881	0.035	340	6.638	…	−3.255	0.51	>0.37
	±0.86	±66	±0.010	±26.5	±0.151	…	±0.060	…	…
HD 71028	1129.5	53846.9	0.147	166.1	4.989	…	34.147	0.41	>0.29
	±3.2	±42.6	±0.028	±14.2	±0.174	…	±0.086	…	…

Table 3. continued.

Name	P (d)	T (+24 00000)	e (deg)	ω_A (km s^{-1})	K_1 (km s^{-1})	K_2 (km s^{-1})	γ (km s^{-1})	rms$_{1,2}$	$M_{1,2}\sin^3 i$ ($\mathcal{M}_\odot$)
HIP 46383	8.490802	57396.839	0.0987	324.3	56.286	57.002	−32.322	0.38	0.63
	±0.000003	±0.013	±0.0016	±0.6	±0.095	±0.096	±0.005	0.43	0.63
HIP 46926	3.10662	54604.7305	0.0	0.0	22.600	26.464	−10.859	0.59	0.020
	±0.00001	±0.0025	fixed	fixed	±0.127	±0.185	±0.065	0.50	0.017
HIP 47133	4.38804	58055.344	0.474	140.2	69.252	74.379	−0.677	2.71	0.47
	±0.00001	±0.015	±0.005	±1.9	±2.035	±2.506	±0.257	2.79	0.44
HIP 47899	146.309	56614.18	0.075	5.8	20.100	21.360	−15.010	0.66	0.55
	±0.020	±1.50	±0.005	±3.6	±0.131	±0.144	±0.071	0.63	0.52
HIP 48346	79.013	56464.52	0.695	187.9	26.408	36.202	−14.648	0.86	0.43
	±0.073	±1.03	±0.041	±2.5	±3.209	±4.602	±0.308	2.82	0.31
HIP 50156	73.225	56288.11	0.140	308.7	9.851	…	8.741	0.63	>0.22
	±0.030	±2.10	±0.027	±11.1	±0.266	…	±0.222	…	…
HIP 50271	47.4632	49595.278	0.688	55.6	28.703	…	4.288	0.98	>0.45
	±0.0003	±0.028	±0.003	±0.6	±0.156	…	±0.108	…	…
HIP 56229	186.3:	58096.59	0.549	345.7	22.183	23.033	12.015	0.42	0.53
	±0.73	±1.04	±0.050	±1.7	±2.298	±2.386	±0.064	0.33	0.51
HIP 57058	725.9	57934.3	0.164	168.0	8.065	…	19.708	0.53	>0.50
	±0.9	±61.7	±0.079	±28.9	±1.128	…	±0.603	…	…
BD+44 2120B	2.22596	55870.6875	0.0	0.0	46.215	…	−4.387	1.15	>0.35
	±0.00001	±0.0038	fixed	fixed	±0.322	…	±0.218	…	…
HIP 61436	299.55	56819.02	0.457	260.7	17.590	19.677	−0.363	0.48	0.49
	±0.18	±1.24	±0.013	±1.9	±0.294	±0.491	±0.135	0.96	0.46
HIP 62755	2238	56347.9	0.140	27.3	8.027	…	−47.032	0.11	>0.69
	±27	±127.6	±0.024	±20.9	±0.419	…	±0.167	…	…
HIP 65026	446.87	57009.7	0.082	12.2	9.129	…	0.109	0.65	0.65:
	±0.43	±10.1	±0.014	±8.4	±0.158	…	±0.104	…	>0.29
HIP 65327	4354.0	56827.0	0.497	115.2	5.030	…	−8.528	0.21	>0.45
	±13.8	±55.8	±0.051	±8.7	±0.557	…	±0.20	…	…
HIP 65887	1200.0	53733.7	0.078	68.6	6.143	…	−3.416	0.45	>0.38
	±3.0	±47.8	±0.020	±14.5	±0.134	…	±0.074	…	…
HIP 66290	1967	51294.7	0.681	78.5	6.731	…	−14.044	0.54	>0.36
	±11	±9.1	±0.018	±5.8	±0.315	…	±0.139	…	…
HIP 67086	40.871	56774.02	0.318	208.9	28.116	33.602	−27.226	0.55	0.46
	±0.007	±0.34	±0.024	±2.8	±0.564	±1.070	±0.255	0.54	0.39
BD+26 2498	1536.2	53208.1	0.190	258.3	12.063	…	−13.641	0.52	>1.02
	±1.8	±15.0	±0.010	±3.5	±0.117	…	±0.100	…	…
BD+19 2735	3616	55769.8	0.607	89.8	4.913	…	−9.535	0.28	>0.34
	±69	±33.2	±0.176	±7.9	±1.566	…	±0.120	…	…
HIP 68801	2.84019	54536.9453	0.0	0.0	86.676	88.273	−36.319	1.10	0.79
	±0.00001	±0.0009	fixed	fixed	±0.173	±0.222	±0.099	0.90	0.78
HIP 69549	6.03150	54087.0820	0.0	0.0	64.754	65.831	8.578	1.13	0.70
	±0.00001	±0.0016	fixed	fixed	±0.132	±0.139	±0.068	1.36	0.69
HIP 76941	267.06	57157.05	0.492	315.3	7.054	…	−12.497	0.38	>0.23
	±0.31	±1.36	±0.012	±1.7	±0.122	…	±0.071	…	…
HIP 77141	17.3120	58299.184	0.836	14.2	50.441	…	−3.460	0.28	>0.34
	±0.0005	±0.070	±0.154	±8.1	±58.975	…	±2.167	…	…
HIP 78158	322.04	57083.48	0.395	299.7	11.784	…	−44.839	0.34	>0.44
	±0.16	±1.43	±0.014	±1.9	±0.219	…	±0.099	…	…
HIP 80751	5252	58096.9	0.188	64.5	3.031	…	−32.748	0.23	>1.02
	±324	±692.7	±0.069	±55.1	±0.748	…	±0.582	…	…
HIP 92952	7.9461	57609.65	0.044	291.9	17.290	…	−18.380	0.40	>0.18
	±0.0002	±0.28	±0.007	±12.8	±0.148	…	±0.133	…	…
BD+77 767	17.3231	56737.1289	0.391	225.5	40.434	…	−25.831	0.32	>0.63
	±0.0002	±0.0329	±0.005	±0.9	±0.331	…	±0.114	…	…
HIP 101941	1026.69	54442.6	0.223	211.8	9.975	…	−20.562	0.43	>0.64
	±1.37	±7.8	±0.012	±2.8	±0.111	…	±0.075	…	…
HIP 102320	21.1854	57143.617	0.416	322.1	40.879	41.954	−21.080	0.30	0.47
	±0.0002	±0.016	±0.003	±0.3	±0.141	±0.206	±0.049	0.19	0.46
HIP 104994	51.82128	55970.823	0.407	303.6	25.796	32.988	−46.869	0.85	0.48
	±0.0015	±0.087	±0.003	±0.9	±0.090	±0.152	±0.062	0.49	0.37

Table 3. continued.

Name	P (d)	T (+24 00000)	e (deg)	ω_A (km s^{-1})	K_1 (km s^{-1})	K_2 (km s^{-1})	γ (km s^{-1})	rms$_{1,2}$	$M_{1,2} \sin^3 i$ ($\mathcal{M}_\odot$)
HIP 110291	764.8	54423.0	0.563	3.9	3.888	...	−108.035	0.52	>0.15
	±3.5	±4.7	±0.028	±4.0	±0.219	...	±0.088	...	...
HIP 111685	6177	54730	0.249	300.1	3.752	...	−58.378	0.33	>0.40
	±26	±22	±0.007	±1.3	±0.154	...	±0.113	...	...
HIP 111942	375.098	56849.88	0.437	339.5	7.880	...	−32.470	0.32	>0.30
	±0.038	±1.39	±0.011	±0.4	±0.080	...	±0.070	...	...
HIP 112523	3255:	55676.2	0.480	190.5	3.871	...	4.154	0.58	>0.36
	±50	±41.7	fixed	±6.2	±0.243	...	±0.156	...	...
BD+66 1664	3.09995	53785.0117	0.0	0.0	23.940	...	−22.083	0.67	>0.18
	±0.00004	±0.0036	fixed	fixed	±0.174	...	±0.123	...	...
HIP 118212	872.90	56678.80	0.536	135.4	8.428	...	0.999	0.36	>0.40
	±1.23	±2.71	±0.016	±2.5	±0.138	...	±0.131	...	...